Elasticité des verres et des liquides surfondus : Spectroscopie Brillouin

Benoit Rufflé

Laboratoire Charles Coulomb
University of Montpellier, France

Outline

- **Introduction**
- Brillouin scattering mechanism
- Instrumentation
- Applications to glasses and melts

Introduction

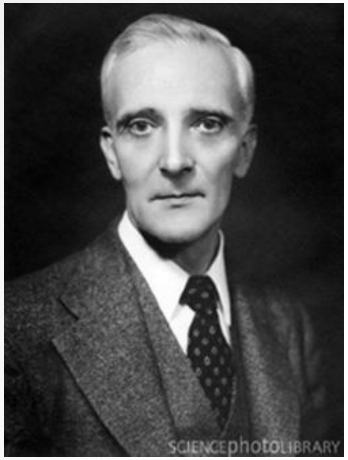

Léon Nicolas Brillouin (1889-1969)

- Brillouin scattering is named after Léon Nicolas Brillouin
- Predicted the inelastic scattering of light (photons) by thermally generated acoustic vibrations (phonons) in 1922

- Leonid Mandelstam is believed to have discovered the scattering as early as 1918, but he published it only in 1926

Leonid Mandelstam (1879-1944)

Acoustic vibrations ?

Diatomic chain

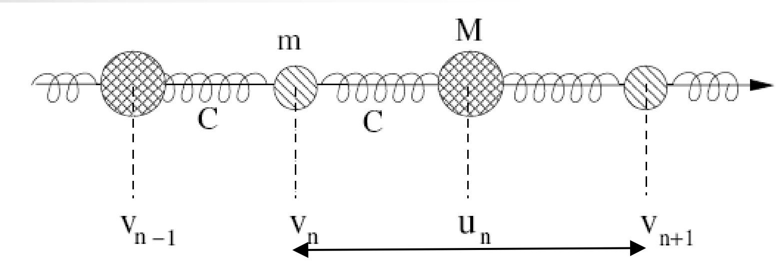

a

Raman scattering

Brillouin scattering

$\omega(k) = v_s k$

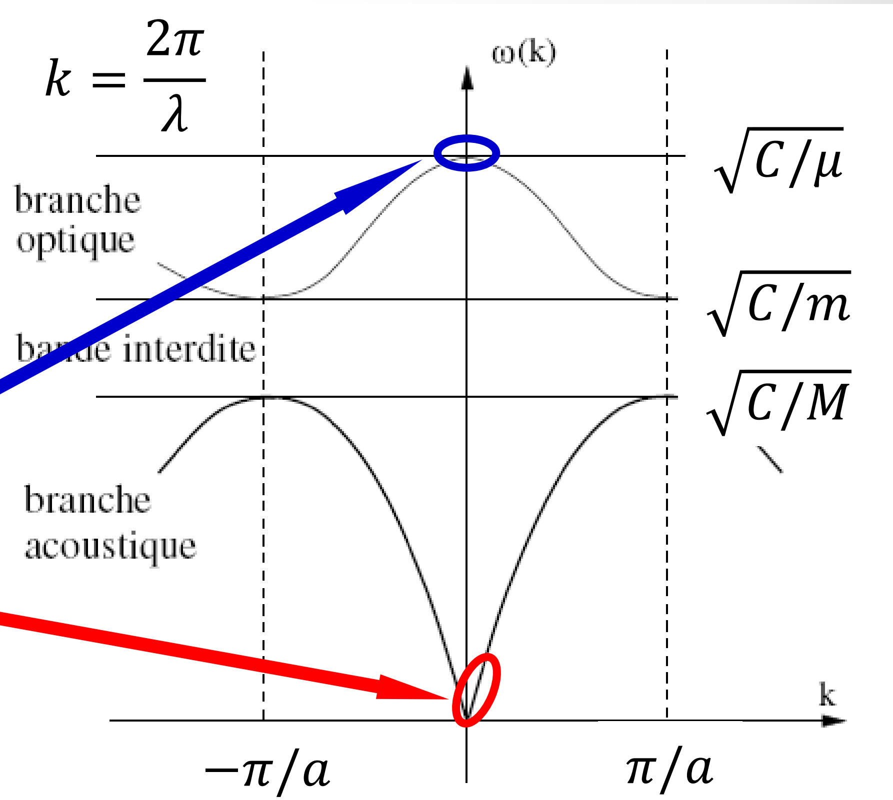

Dispersion relation $\omega(k)$

3D
- 3 acoustic branches (1L, 2T)
- 2 in isotropic materials (T_1=T_2)
- 1 in "fluids"

Polarization of modes

Longitudinal acoustic 1D mode

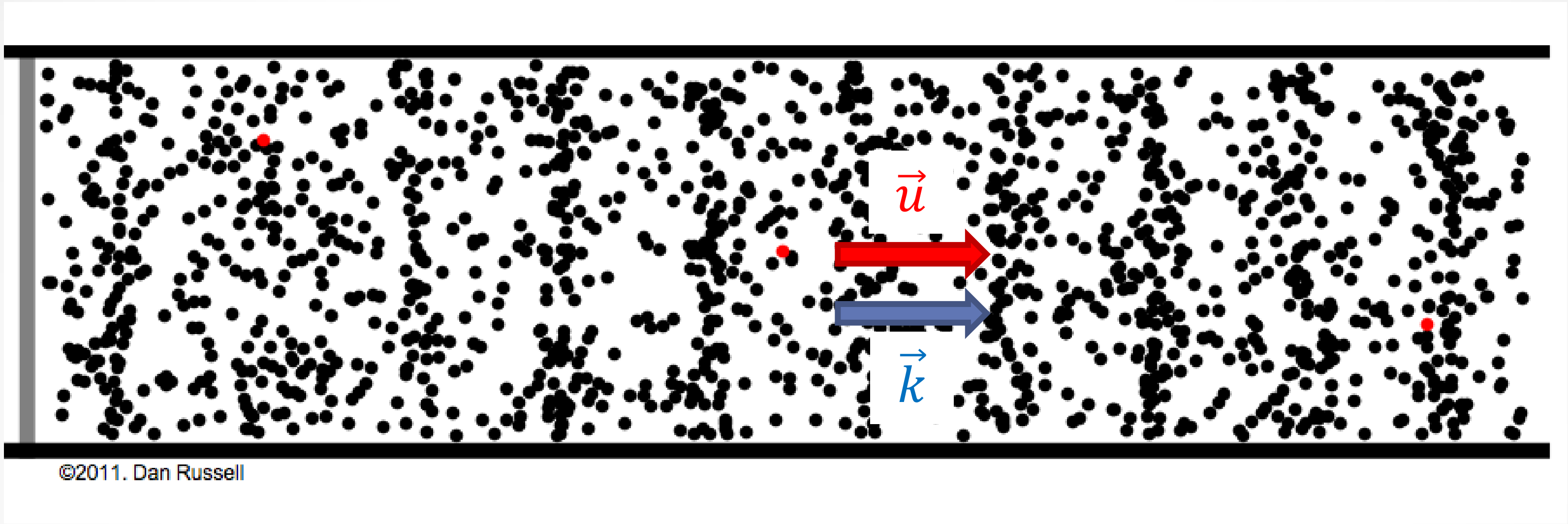

Transverse acoustic 1D mode

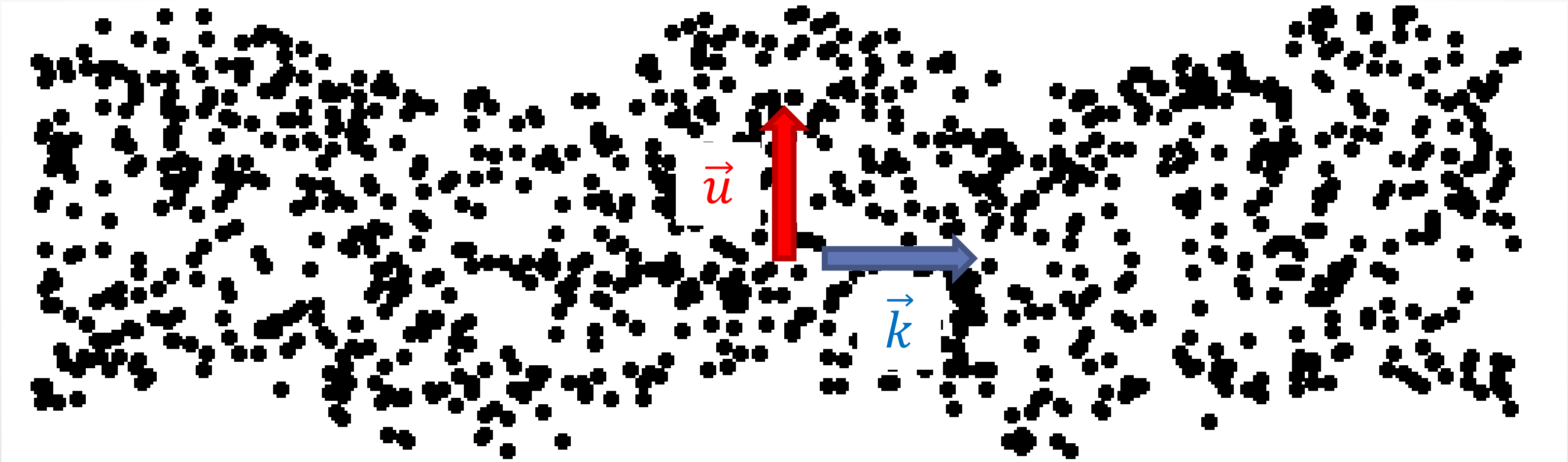

Elasticity of continuous media

Macroscopic properties (ρ, elastic constants C_{ijkl})

- continuum linear elasticity
- stress proportional to strain $\sigma_{ij} = C_{ijkl}\varepsilon_{kl}$

  (nonpiezoélectric media)
- plane-wave solution of the equation of motion
- secular equation $\left|C_{ijkl}\hat{q}_j\hat{q}_k - \varrho v^2\delta_{il}\right| = 0$
  - 3 solutions v for each $\vec{q}$ direction
  - eigenvectors $\perp$, sound velocities v, modules ρv^2
  - high symmetry direction (1L+2T)
  - other (1QL+1QT+1T)
- Piezoelectric media $\sigma_{ij} = C_{ijkl}\varepsilon_{kl} - e_{mij}E_m$

  $\Rightarrow C_{ijkl}(\vec{q})$

Outline

- Introduction
- **Brillouin scattering mechanism**
- Instrumentation
- Applications to glasses and melts

Classical view

Diffraction grating produced by periodic density variations (refraction index changes)

Bragg reflection

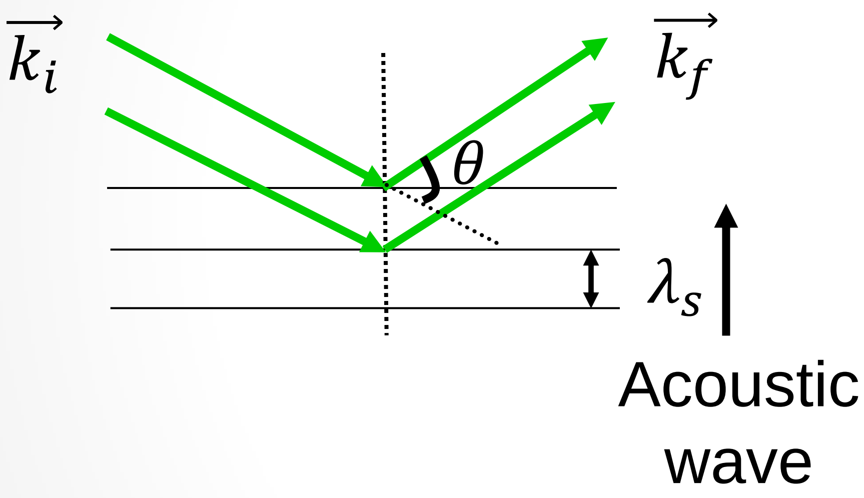

$$2\lambda_s \sin\frac{\theta}{2} = \frac{\lambda_0}{n}$$

Doppler effect

$$\nu_B = \frac{v_s}{\lambda_s} = \frac{2nv_s}{\lambda_0}\sin\frac{\theta}{2}$$

Brillouin Shift

Quantum view

inelastic photon-phonon interaction

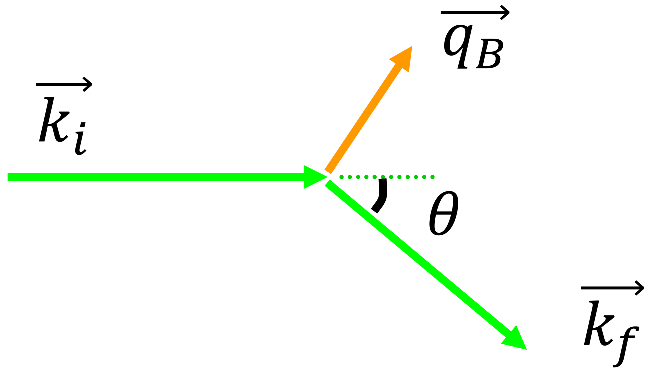

Stokes/anti-Stokes process

$$\overrightarrow{k_f} - \overrightarrow{k_i} = \pm \overrightarrow{q_B}$$

$$\omega_f - \omega_i = \pm \omega_B$$

Low energy transfer $|\overrightarrow{k_i}| \sim |\overrightarrow{k_f}|$ $(\omega_B/\omega_i \sim v_s/c \sim 10^{-5})$

$$\left.\begin{array}{l} q_B = 2k_i \sin\frac{\theta}{2} \\ \omega_B = v_s q_B \end{array}\right\} \nu_B = \frac{\omega_B}{2\pi} = \frac{2nv_s}{\lambda_0}\sin\frac{\theta}{2}$$

Brillouin light scattering in a nutshell

- Scattering of incident light from the long-wavelength thermal acoustic modes in a solid

- Scattered light is frequency shifted:
  - sound velocity/refractive index
  - elastic modulus/density

- Spectra give Brillouin frequency shifts and linewidths
  or sound velocities and sound attenuation coefficients
  or complex modulus/viscoelastic properties

- $\lambda >> a \Rightarrow$ continuum elastic media

Outline

- Introduction
- Brillouin scattering mechanism
- **Instrumentation**
- Applications to glasses and melts

Which spectrometer ?

$\lambda_0 \sim \mu\text{m}$
$v_s \sim \text{kms}^{-1}$ → $\nu_B \sim 10\ \text{GHz} \sim 0.3\ \text{cm}^{-1}$ → Fabry–Perot interferometer

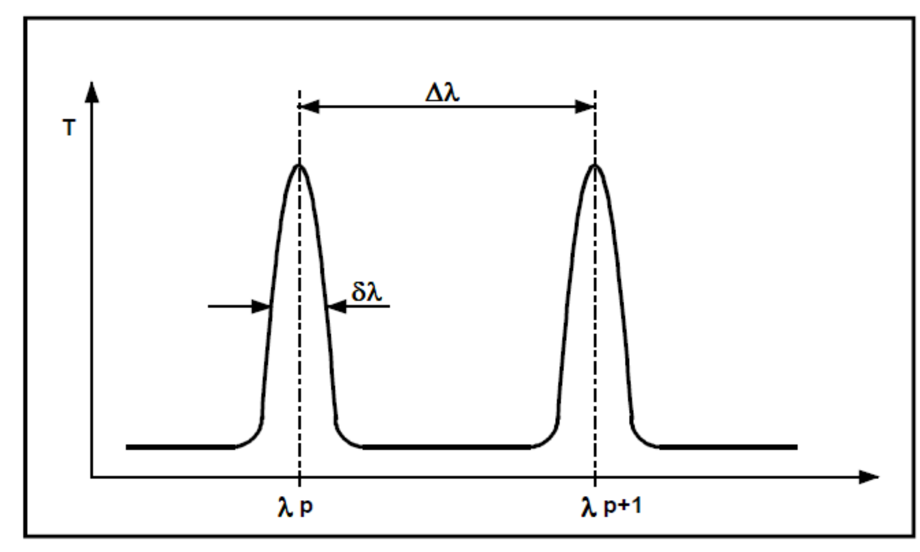

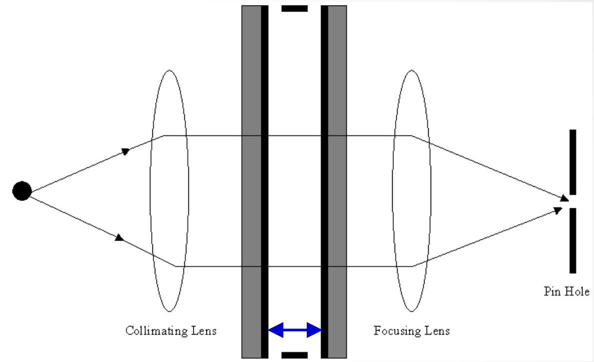

$$T = \frac{T_0}{1 + (4F^2/\pi^2)\sin^2(2\pi L_1/\lambda)}$$

$$T = T_0 \text{ for } L_1 = p\frac{\lambda}{2}$$

$R = 0.94$

Finesse: $F = \Delta\lambda/\delta\lambda \sim 50$ Contrast: $C = 4F^2/\pi^2 \sim 10^3$

Free Spectral Range: $FSR(\text{GHz}) = 150/L_1(\text{mm})$

$I_B \sim 10^{-12} I_0$ Incident flux

Standard Brillouin spectrometer

Tandem setup (Sandercock 1976) => Vernier system

High contrast (6 pass), good resolution, versatile spectrometer

$$L_1 = p\frac{\lambda}{2} \quad L_2 = q\frac{\lambda}{2}$$

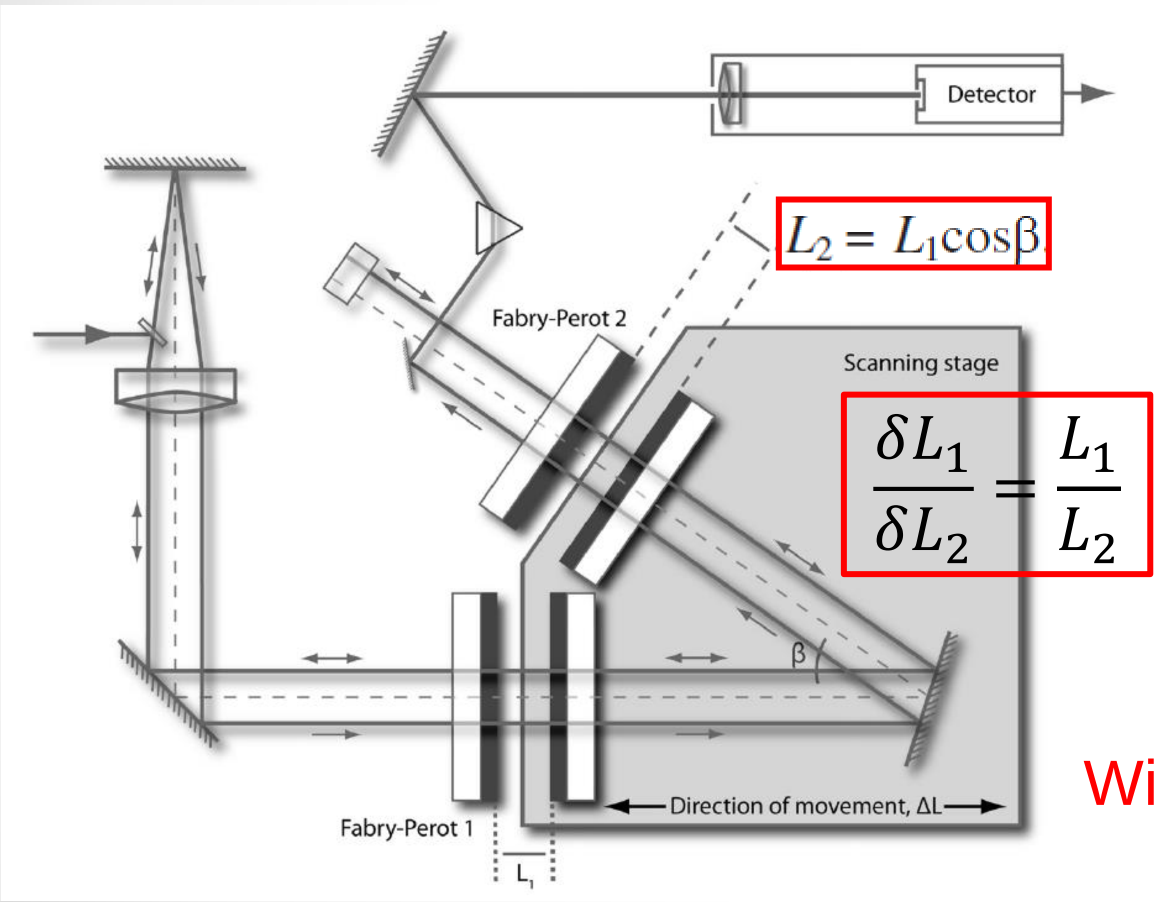

$$L_2 = L_1 \cos\beta$$

$$\frac{\delta L_1}{\delta L_2} = \frac{L_1}{L_2}$$

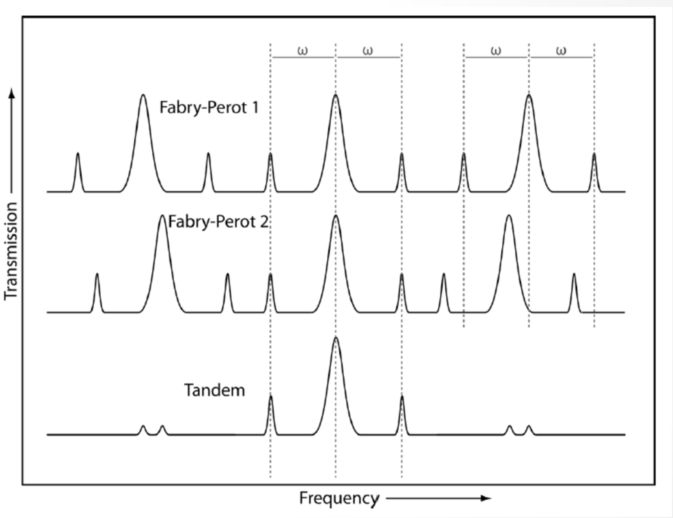

Within 2 nm!

Tandem Fabry-Perot interferometer

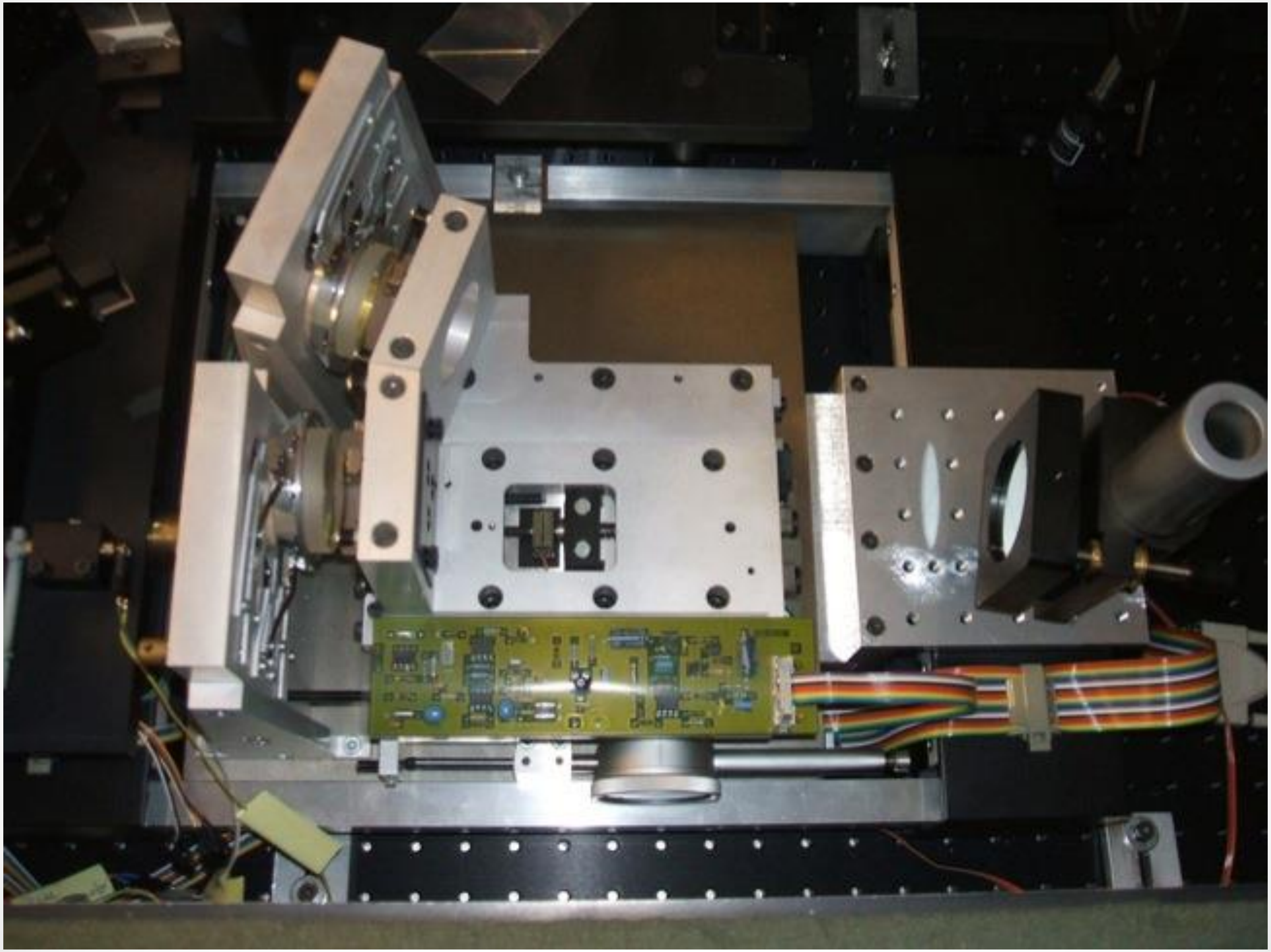

Typical setup

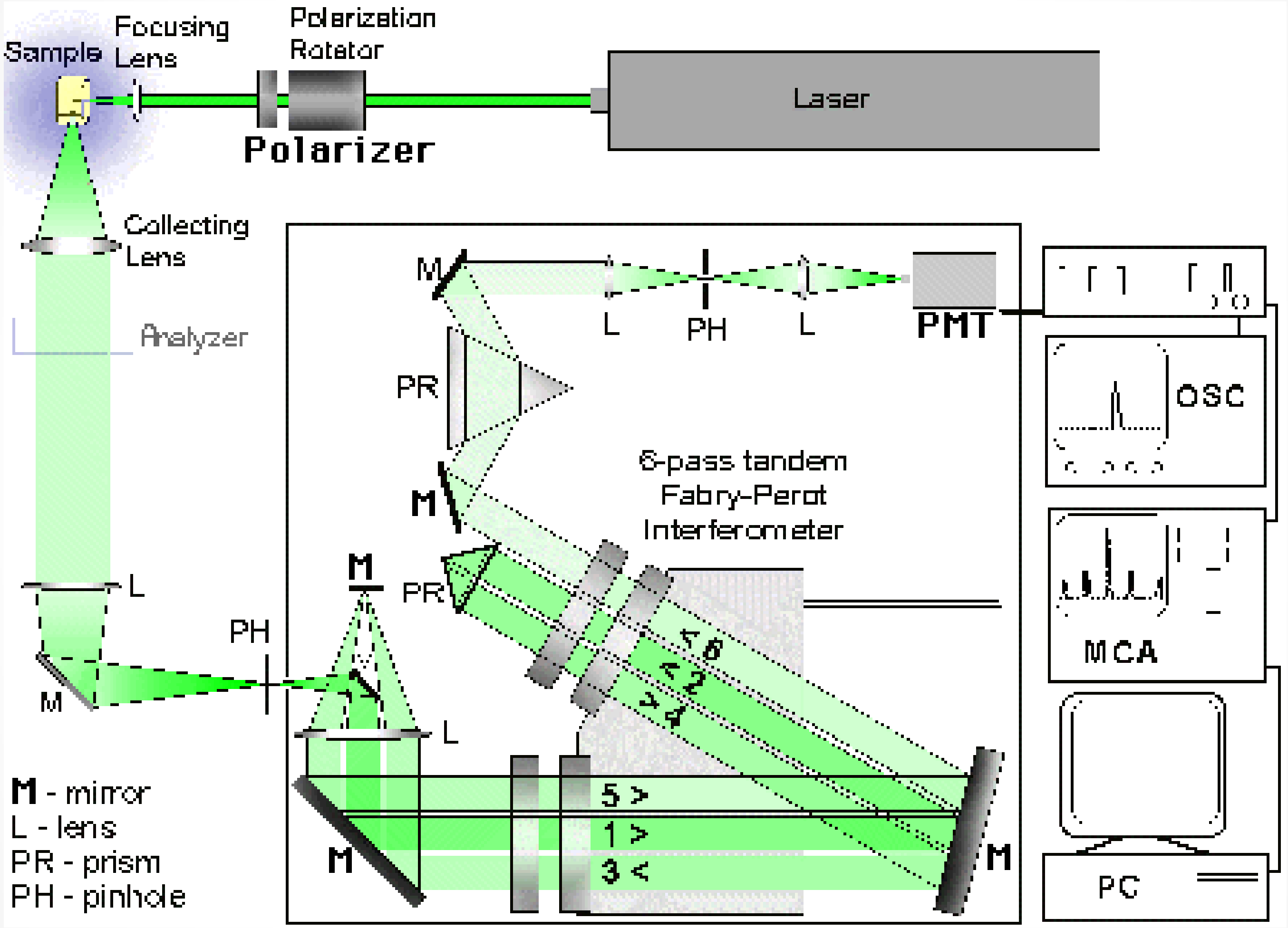

Schematic Brillouin spectrum

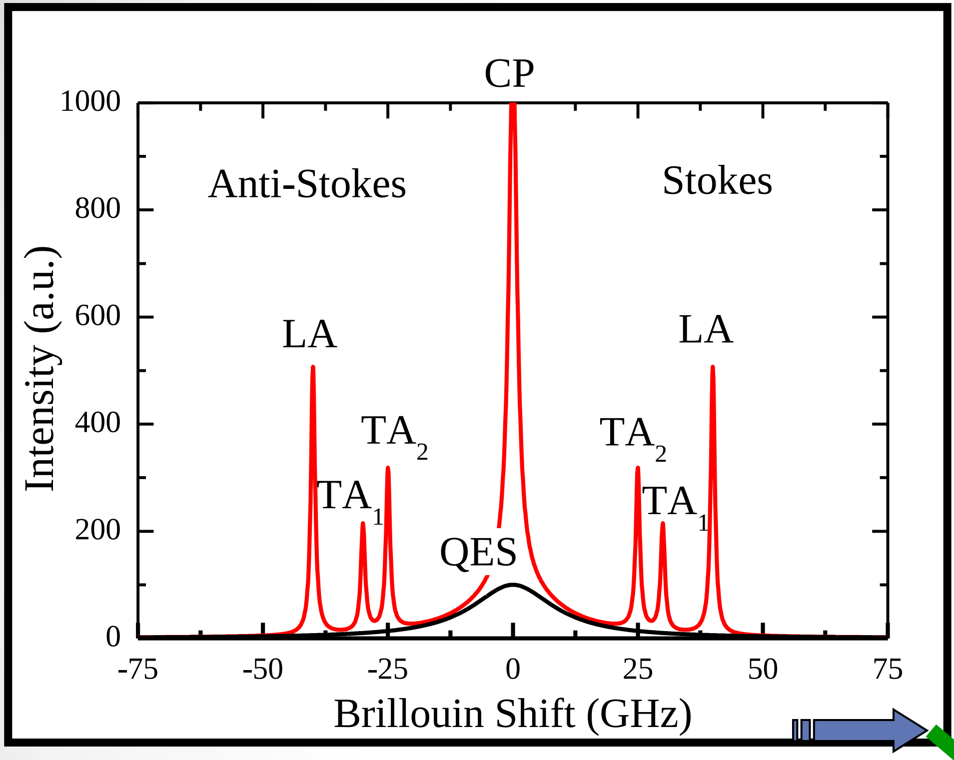

- Temporal fluctuations $\delta\kappa(\mathbf{r},t)$
  - propagative (vibrations)

    $\Rightarrow$ Raman, Brillouin
  - non propagative

    $\Rightarrow$ quasielastic diffusion
- Static fluctuations $\delta\kappa(\mathbf{r})$

  $\Rightarrow$ Elastic scattering (defects…)

Raman scattering

$\Delta\nu \geq 300$ GHz

(10 cm^{-1})

Visible $\lambda \approx 0.5\ \mu m$, $q \approx 0.04\ nm^{-1}$

- $\nu_B \approx 1 - 100$ GHz (0.03 – 3 cm^{-1})
- $\Gamma = \dfrac{\alpha V}{2\pi}$ (MHz - GHz)

High resolution Brillouin spectrometer

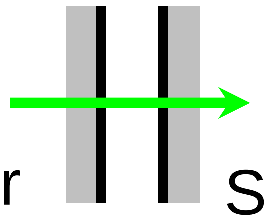

4-pass PFP interferometer
⇒ high contrast C ~ 10^{10}

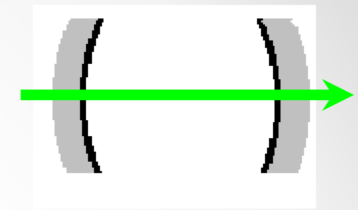

SFP interferometer 50mm
⇒ high resolution 25 MHz

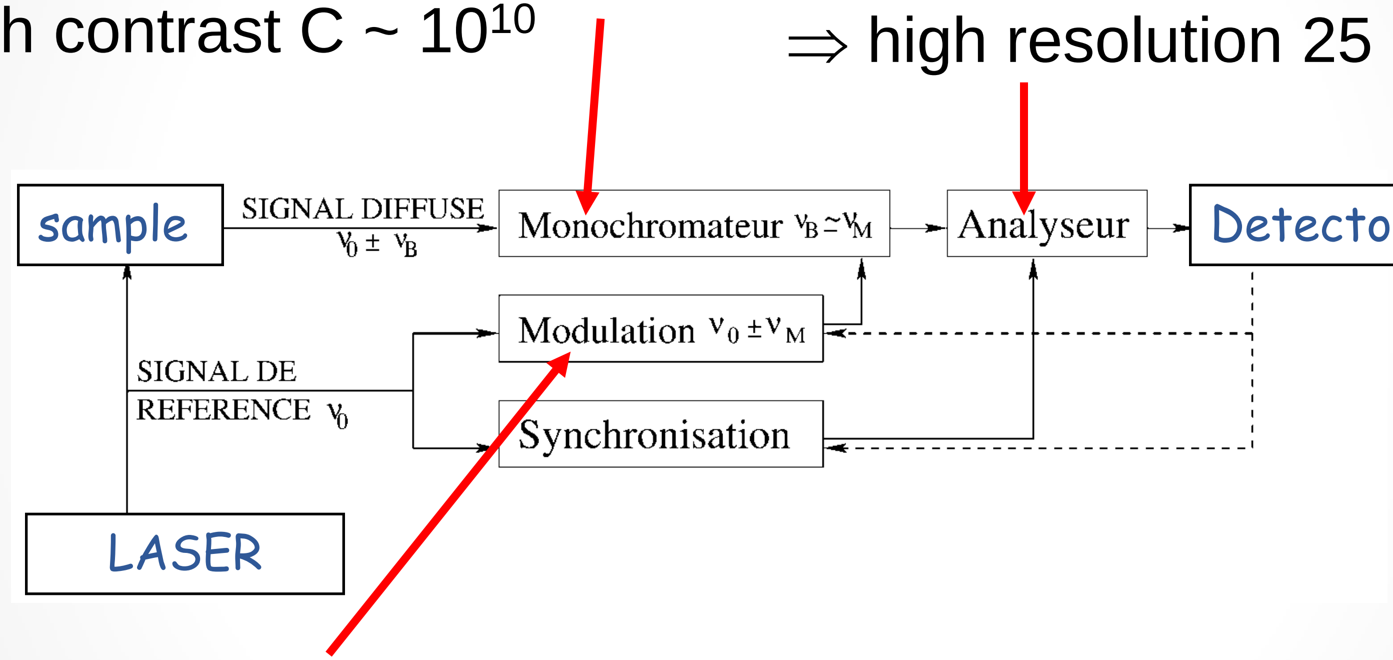

Electro-optic modulation
⇒ high accuracy (~10^{-4}) and high stability

Scattering geometries

Backscattering

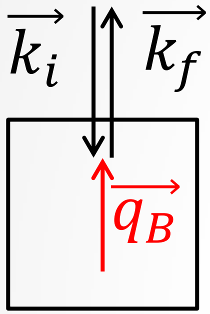

$$\nu_B = \frac{2n v_s}{\lambda_0}$$

$$\frac{\delta \nu_B(\theta)}{\nu_B(\theta)} = \frac{1}{2\tan\frac{\theta}{2}} \sim 0$$

TA inactive in isotropic systems

90° scattering

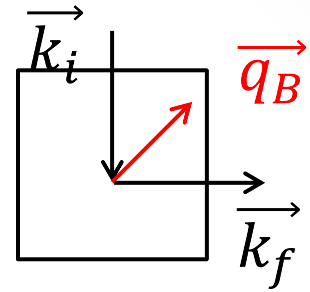

$$\nu_B = \frac{\sqrt{2} n v_s}{\lambda_0}$$

LA and TA

Symmetric platelet

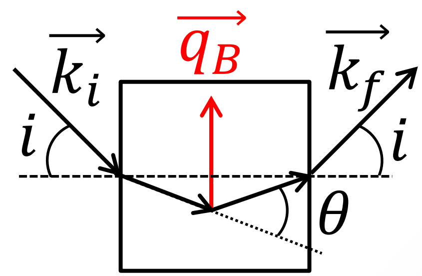

$$\nu_B = \frac{2 v_s}{\lambda_0} \sin i$$

n independent LA and TA

Pros and cons

- Non-contact probe for the viscoelastic properties
  - Non-destructive
  - directional (anisotropy of moduli, stress…)
  - high temperature (melt)
  - high pressure (Diamond anvil cell)

- Small samples or small scattering volume (~ 10 μm^3)
  - μ-Brillouin
  - cartography

BUT

- sample must be transparent
- only nv_s is usually measured (need ρ to get C_{ij})
- small frequency range (1 decade)

  $\lambda_{ac} \sim \mu m$, $q \sim 0.005\text{-}0.05\ nm^{-1}$

Outline

- Introduction
- Brillouin scattering mechanism
- Instrumentation
- **Applications to glasses**

Elastic properties of glasses

- 2 independent elastic constants $C_{12} = C_{11} - 2C_{44}$
- $\lambda = C_{12}$, $\mu = C_{44}$
- $G = C_{44}$ Shear modulus
  $B = C_{11} - 4/3\ C_{44}$ Bulk modulus
- Young modulus *E* and Poisson's ratio ν

Sound velocities

longitudinal acoustic mode transverse acoustic mode

$$v_{LA} = \sqrt{\frac{B + 4G/3}{\rho}} \qquad v_{TA} = \sqrt{\frac{G}{\rho}}$$

Composition trends

$X^{2+}_{2/n}O^{2-} - Al_2O_3 - 2SiO_2$ alumino-silicate glasses

Platelet geometry
300 K

$$\nu = \frac{1}{2}\frac{(\nu_{B_L}^2 - 2\nu_{B_T}^2)}{(\nu_{B_L}^2 - \nu_{B_T}^2)}$$

$$M = C_{11} = \rho v_L^2$$

$$G = C_{44} = \rho v_T^2$$

$$K = \frac{M}{3}\frac{1+\nu}{1-\nu}$$

$$E = 2G(1+\nu)$$

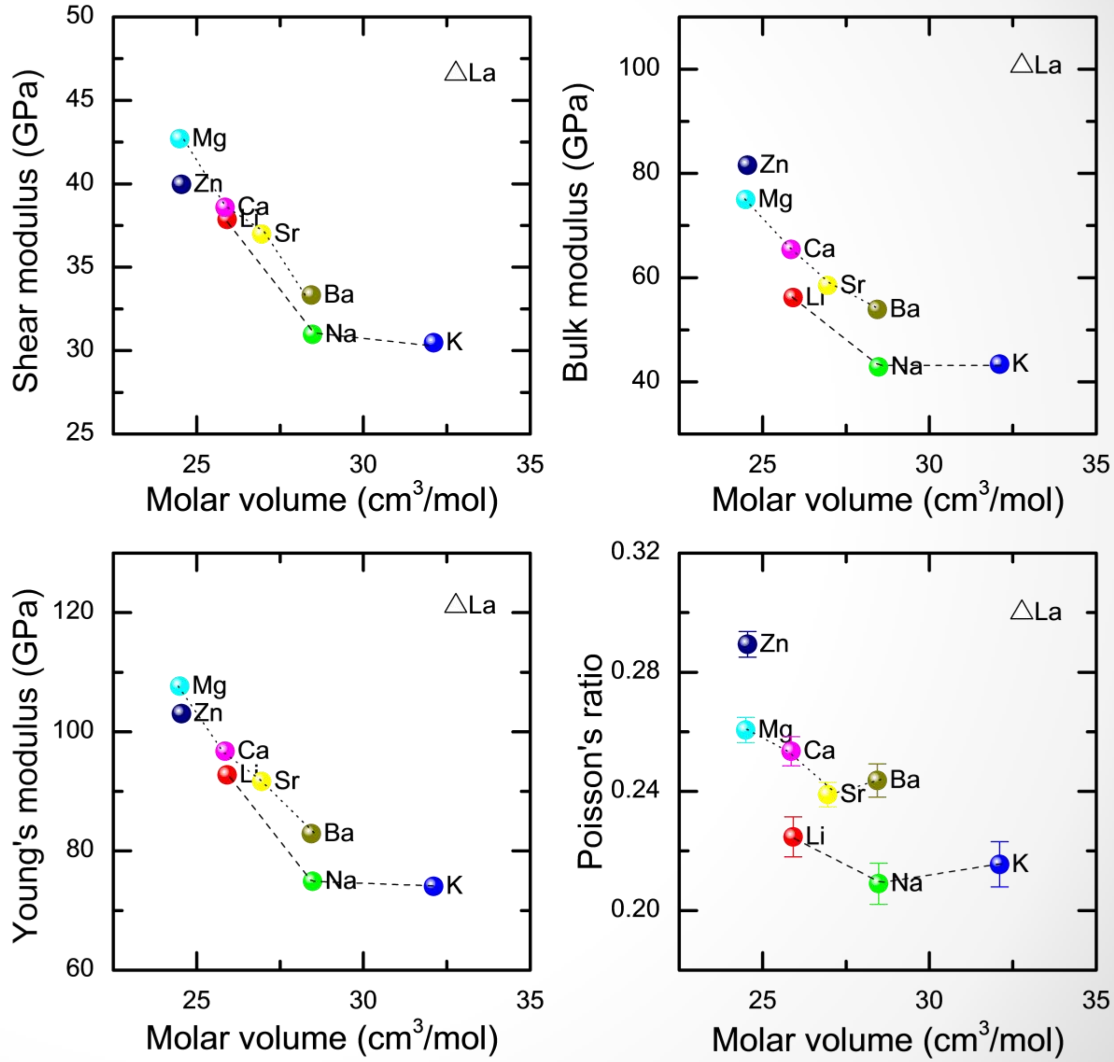

Acoustic modes ⇔ complex elastic moduli

sound velocity: $v(\Omega, T)$

$\delta v/v = (v(\Omega,T) - v_0)/v_0$

↳ (velocity changes)

sound attenuation: $\ell^{-1} = \alpha = \Gamma/v$

$Q^{-1} = \Gamma/\Omega$

↳ (internal friction)

$-2\delta v/v$ and Q^{-1} are Kramers-Krönig transforms of each other

⇒ Measured in sonic, ultrasonic, and hypersonic experiments

Hypersonics:

mainly Brillouin scattering spectroscopies with visible, UV, or x-rays

ν_B ~ 10 GHz - 1 THz , λ_s ~ 0.2 mm – a few nm

Kramers-Kronig relation

If Q^{-1} is small and $v_0 = v_\infty = v(\Omega \to \infty, T)$

Then Q^{-1} and $-2\delta v/v$ are Kramers-Kronig Transforms

$$-2\delta v(\Omega, T)/v \;=\; \frac{1}{\pi}\, P \int_{-\infty}^{+\infty} \frac{Q^{-1}(x,T)}{x-\Omega}\, dx$$

Debye relaxation

$$Q^{-1}(\Omega, T) = A\Omega\tau/(1+\Omega^2\tau^2)$$

$$-2\delta v(\Omega, T)/v = A/(1+\Omega^2\tau^2)$$

Kramers-Kronig relation

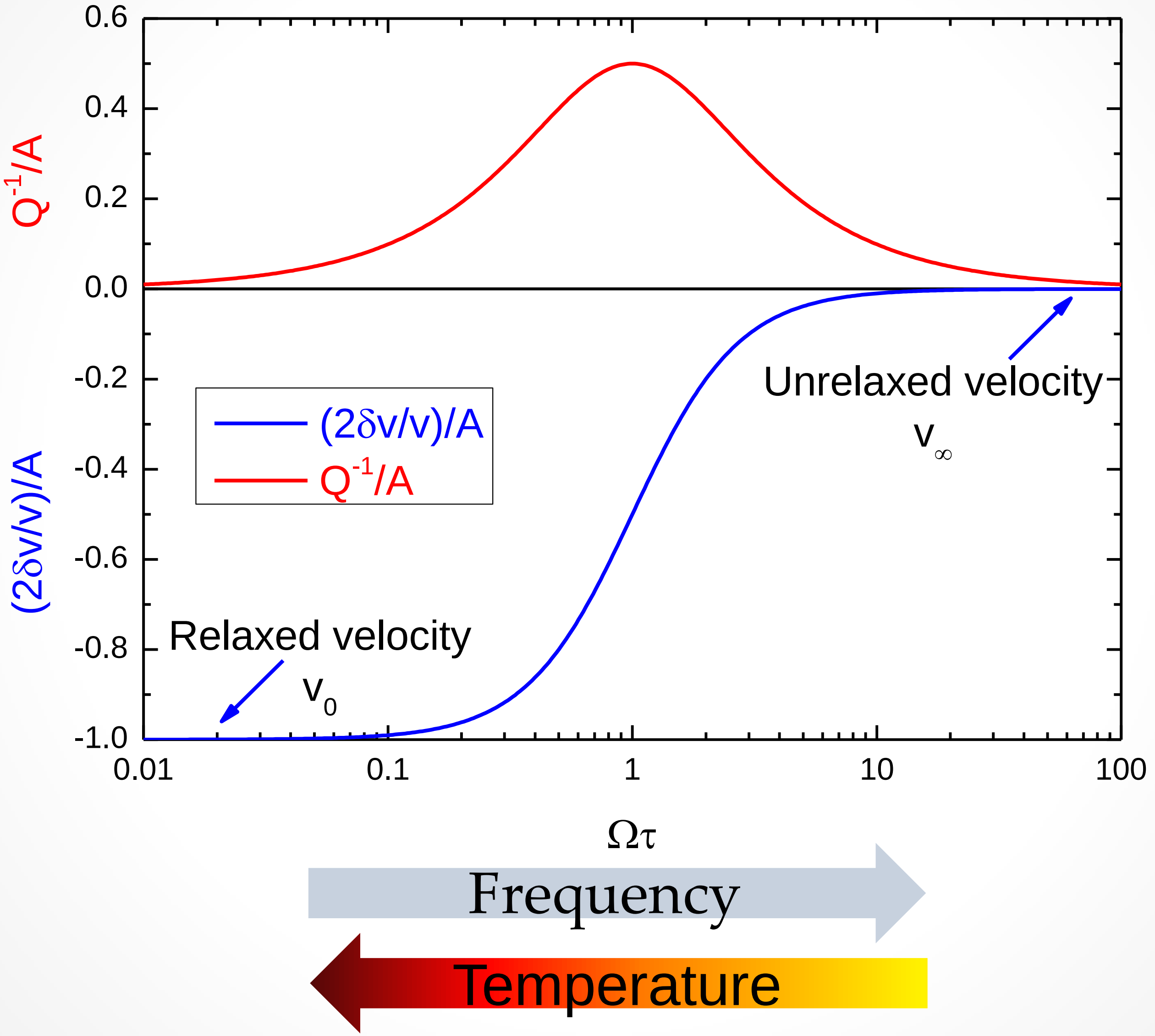

Sound velocity in glasses

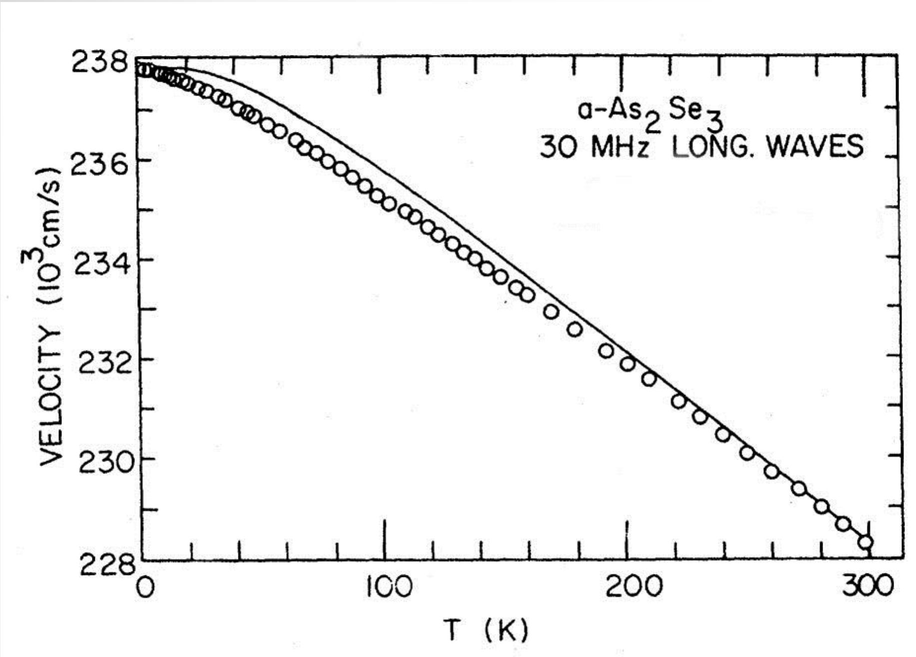

Claytor et al., PRB 1978

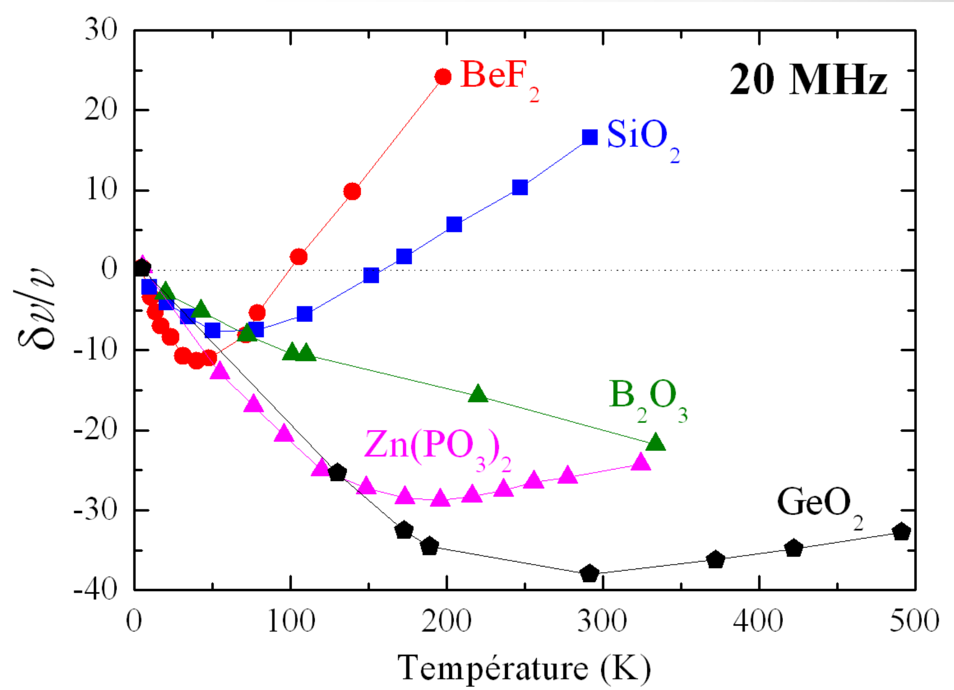

Krause et al. J. Am. Cer. Soc .1968

For some glasses,
very similar to crystals

In many cases, very
anomalous behavior

Sound attenuation in glasses

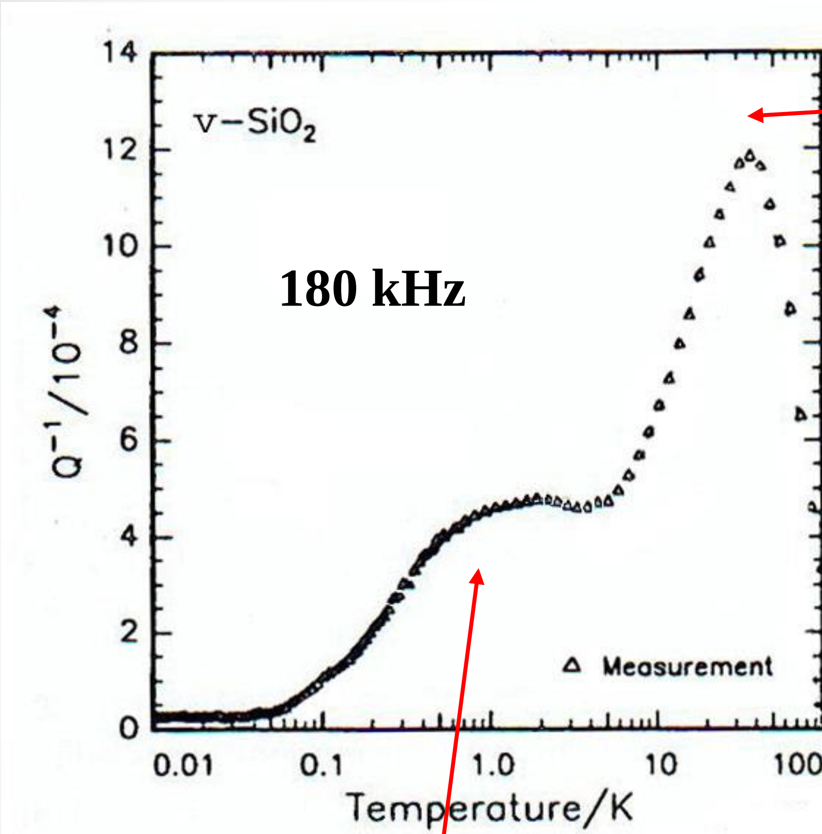

Keil et al., JNCS 1993

Strong damping already at very low T (Two-level systems)

Above 10 K: strong peak in the T-dependence of sound damping in most glasses

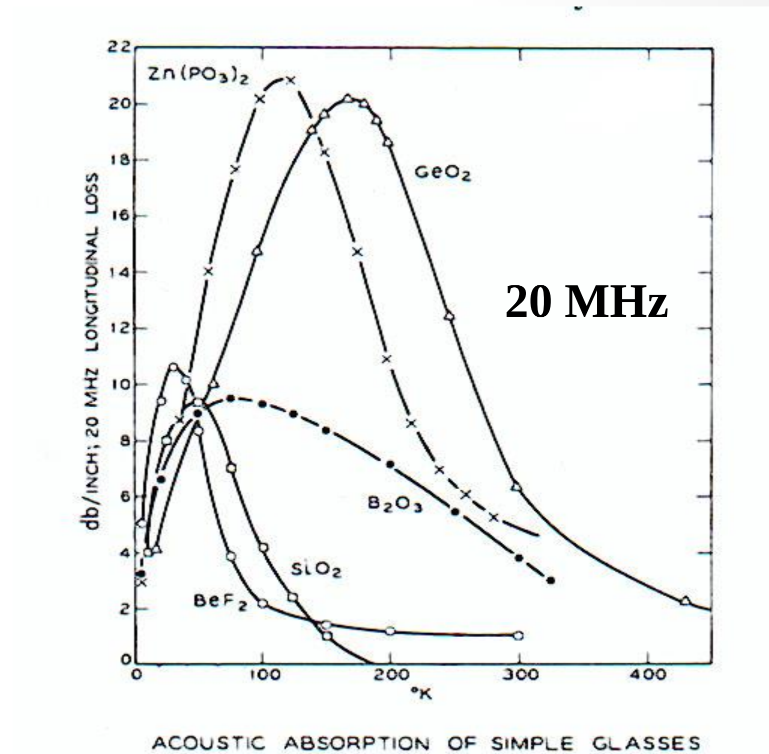

Krause et al., J. Am. Cer. Soc.1968

Damping mechanisms in glasses

From sonic to hypersonic frequencies, two main mechanisms:

- anharmonicity ($\Gamma \propto \Omega^2$) [J. Fabian 1999, R. Vacher 1981, 2005]

  (interaction with the thermally excited modes,

  main mechanism of attenuation in crystals)

- thermally activated relaxations (TAR) [J. Jäckle,S. Hunklinger, 1976]

  (structural defects relaxing in the strain field of the sound wave)

The attenuation peak of glasses

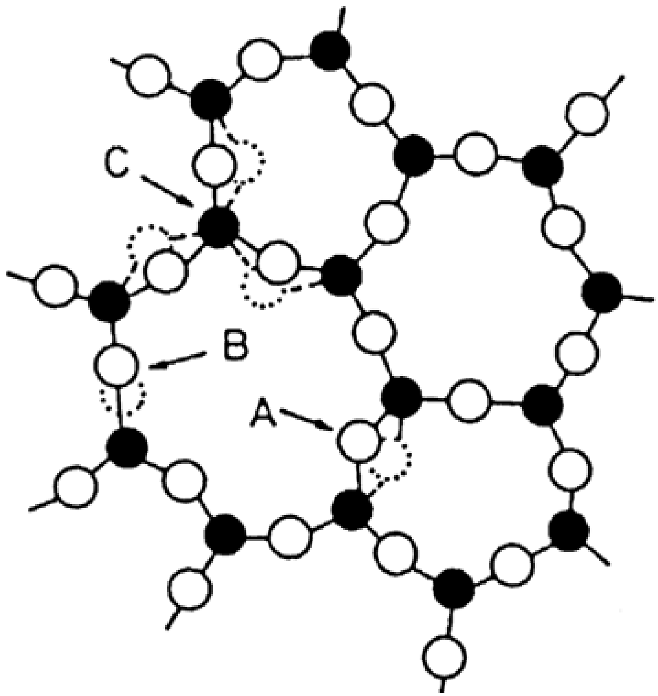

Thermally Activated Relaxation of structural units in asymmetric double-well potentials

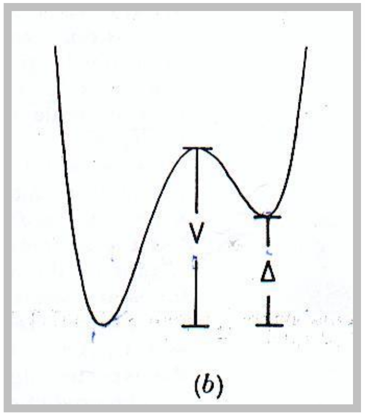

Hunklinger & Arnold, Physical Acoustics 1976

Frequency dependence and shape of the peak
⇨ distribution of barrier heights and asymmetries

$$Q_{\mathrm{rel}}^{-1} = \frac{\gamma^2}{\rho v^2 T} \int_{-\infty}^{\infty} d\Delta \int_0^{\infty} dV \; P(\Delta, V) \,\mathrm{sech}^2 \frac{\Delta}{2T} \frac{\Omega\tau}{1+\Omega^2\tau^2}$$

Revisiting TAR in the silica case, ultrasonic frequencies

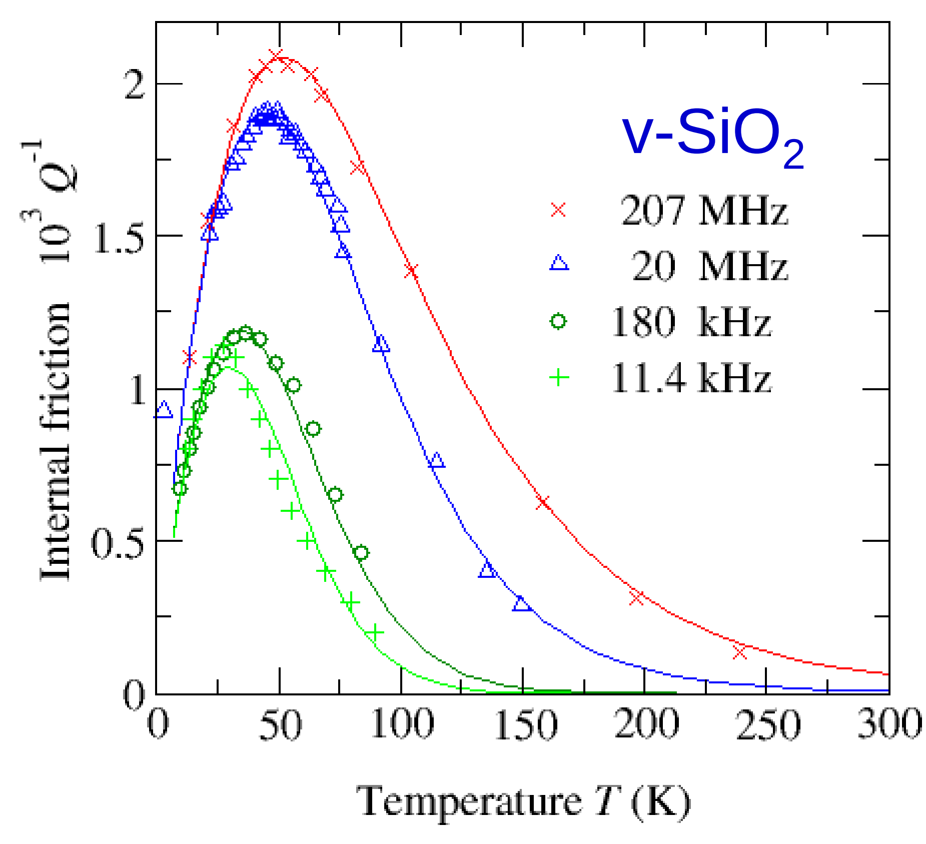

Distribution of barrier heights and asymmetries

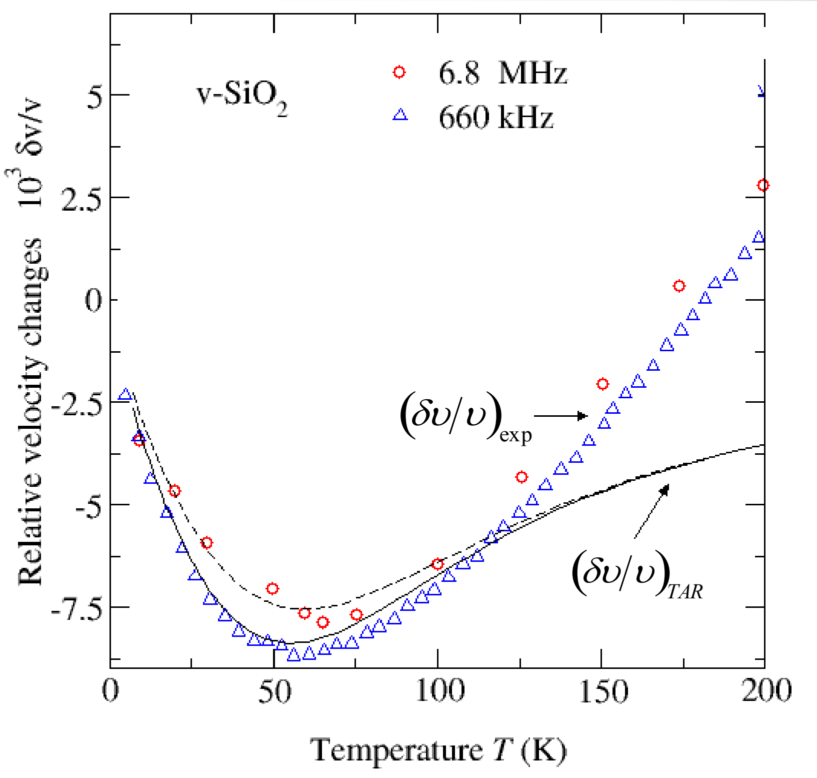

TAR accounts for the dip around 50 K

Damping at hypersonic frequencies

$v\text{-}SiO_2$, 35 GHz

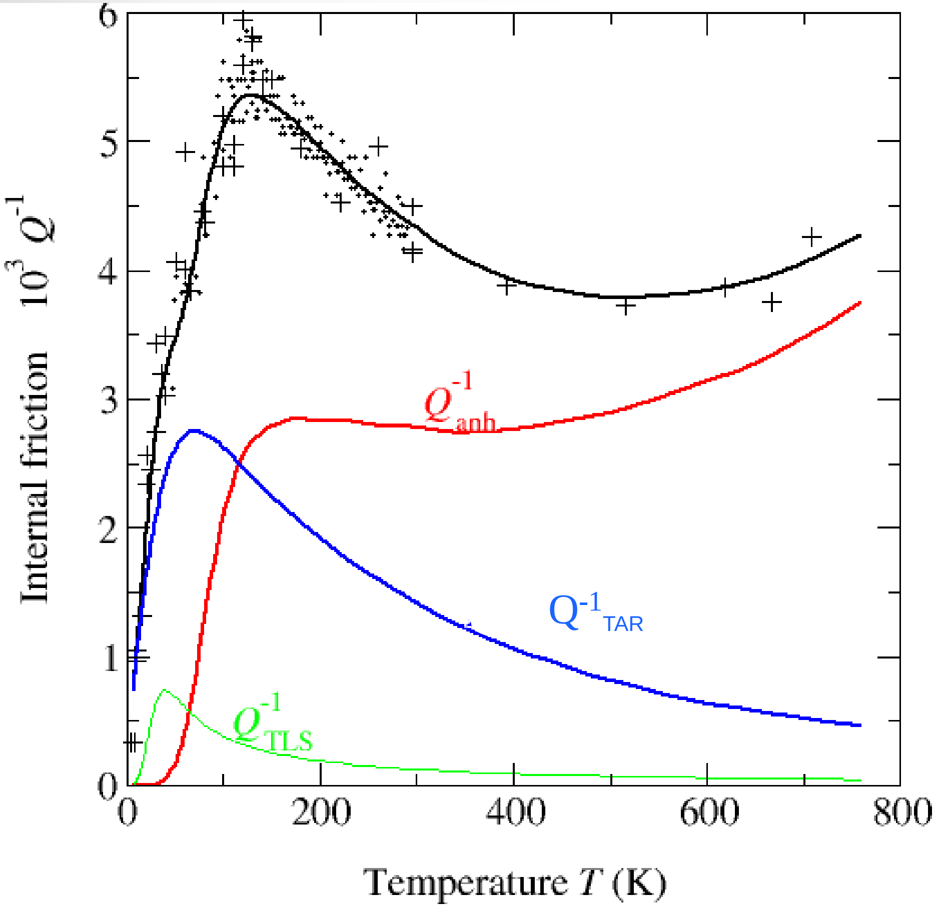

[Vacher, PRB 2005]

Brillouin light scattering:
at high frequency TAR cannot account for the total Q^{-1} in $v\text{-}SiO_2$

Excess explained by anharmonicity

$$Q^{-1}_{anh} = \frac{A\Omega\tau_{th}}{1+\Omega^2\tau^2_{th}}$$

[Maris, PRB 1969]

$$Q^{-1} = Q^{-1}_{anh} + Q^{-1}_{TAR}$$

⇒ Anharmonicity becomes dominant at high Ω

T-dependence of sound velocity in v-SiO_2

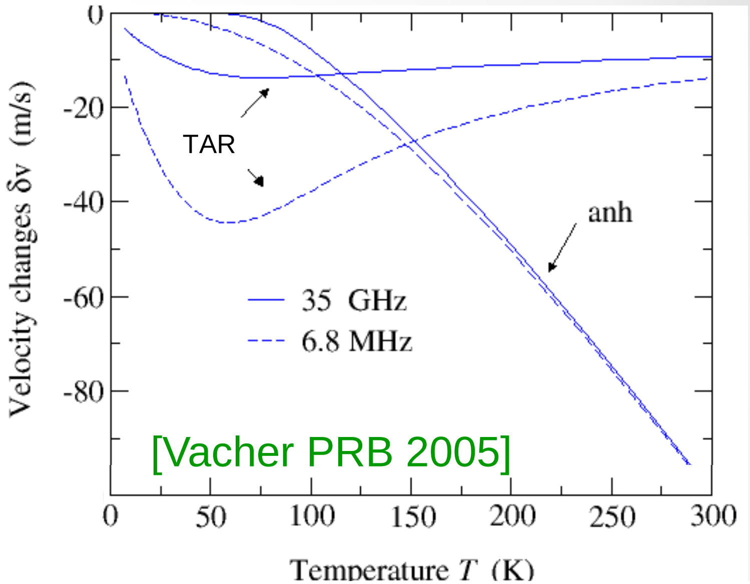

Calculated velocity changes with *T* (TAR and anharmonicity)

Unrelaxed velocity v_∞ is calculated:

$$\upsilon_\infty = \upsilon_{\exp} - \left(\delta\upsilon_{TAR} + \delta\upsilon_{anh}\right)$$

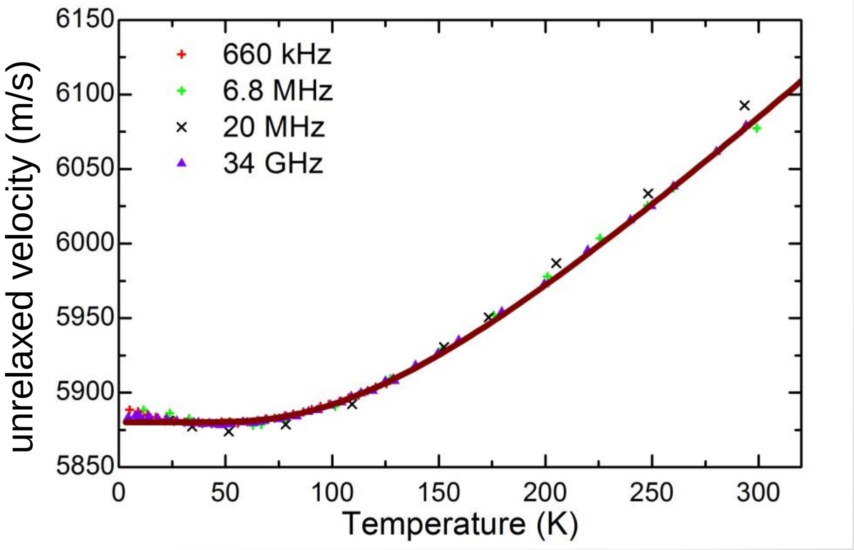

⇒ υ_∞ not constant

⇒ υ_∞ (T) shows anomalous increase

hardening of the structure with increasing *T*

Pressure dependence

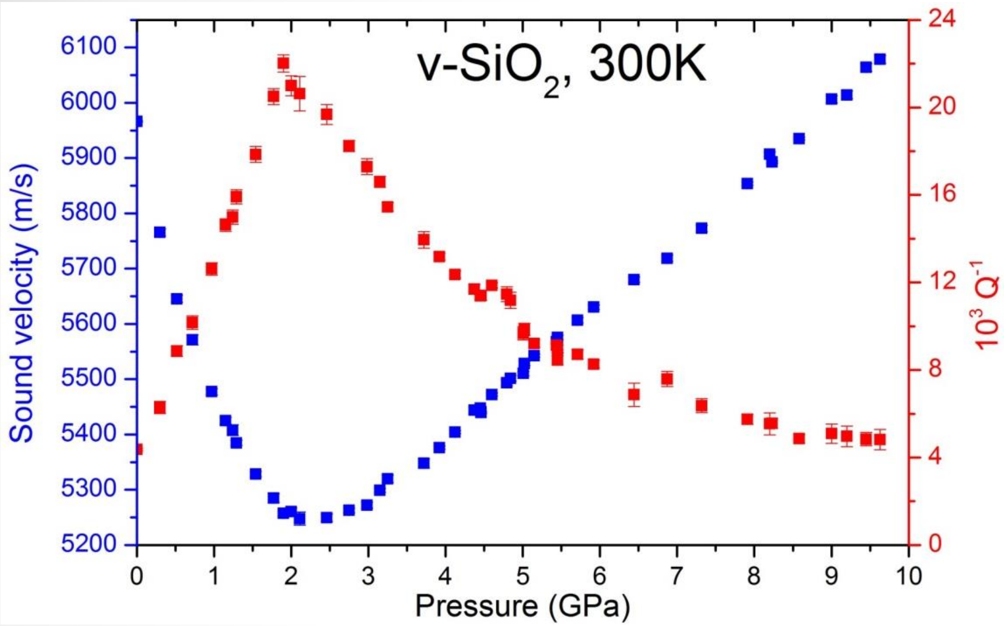

- softening of the structure with P up to 2 GPa
- maximum in Q^{-1} occurs at $v_{\min}$

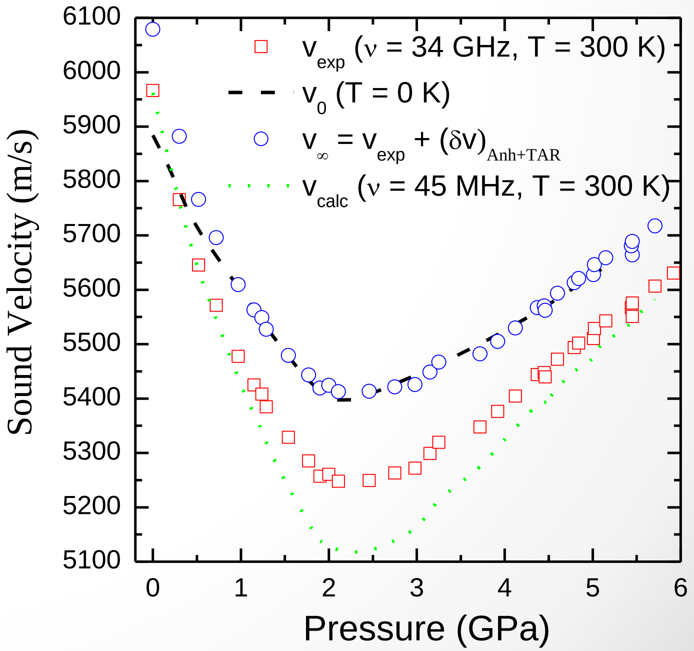

Outline

- Introduction
- Brillouin scattering mechanism
- Instrumentation
- **Applications to highly viscous liquids around Tg**

GeO_2 [G. Guimbretière PhD]

Linkam TS1500 heating stage - backscattering

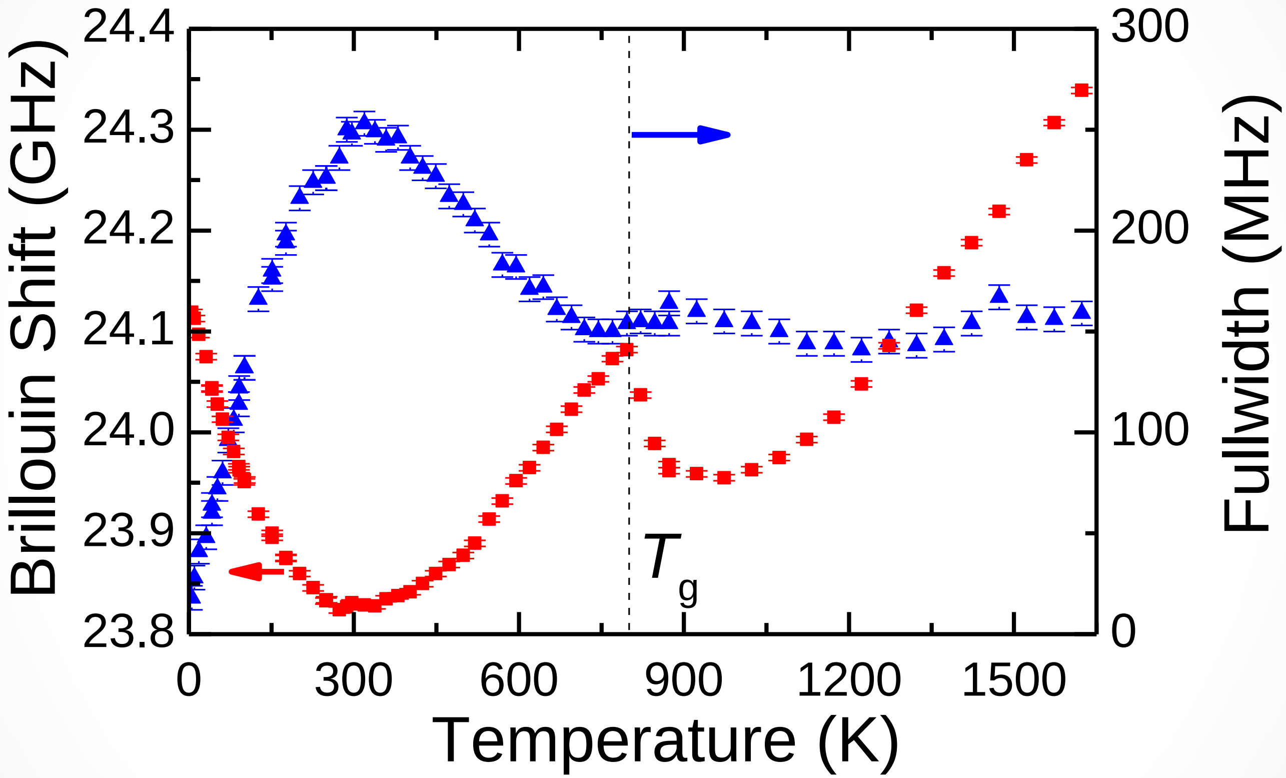

GeO_2 [G. Guimbretière PhD]

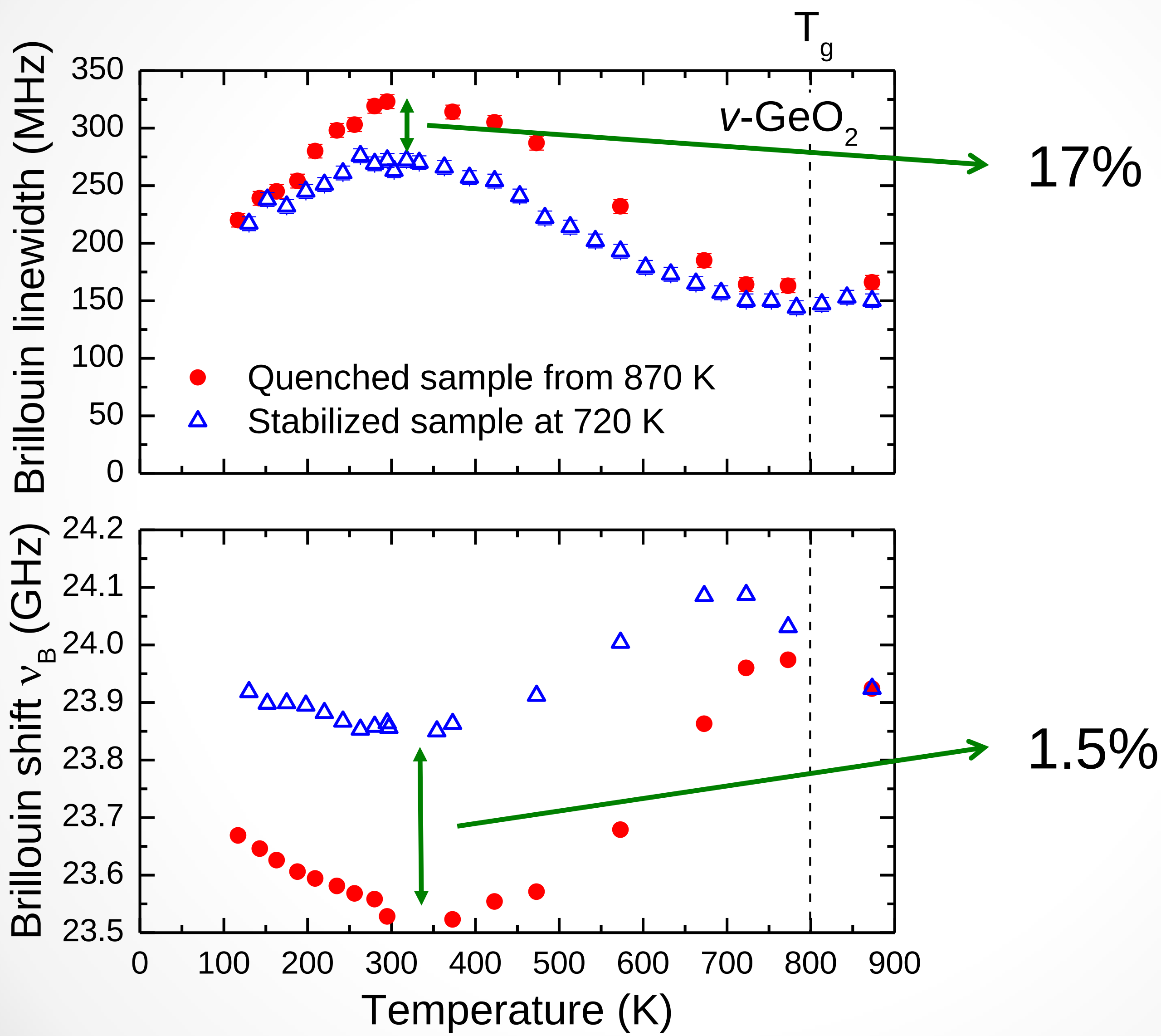

SiO_2 [A. Polian *et al* EPL 2000]

- iridium heating wire in air
  90° geometry
- n from comparison with US
- R from thermal expansion coefficient

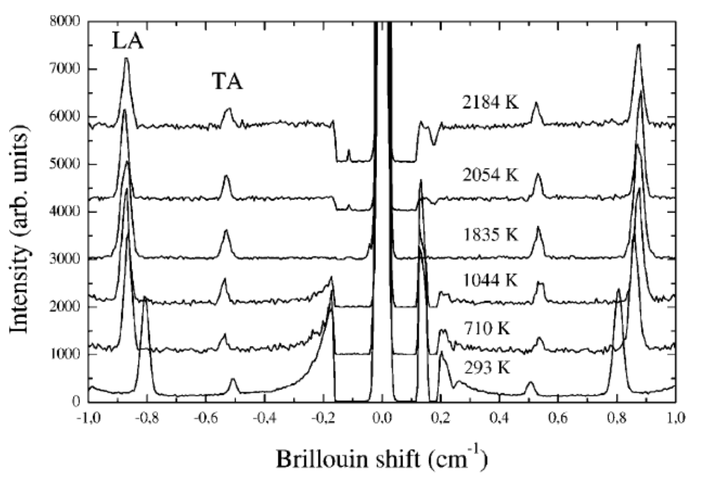

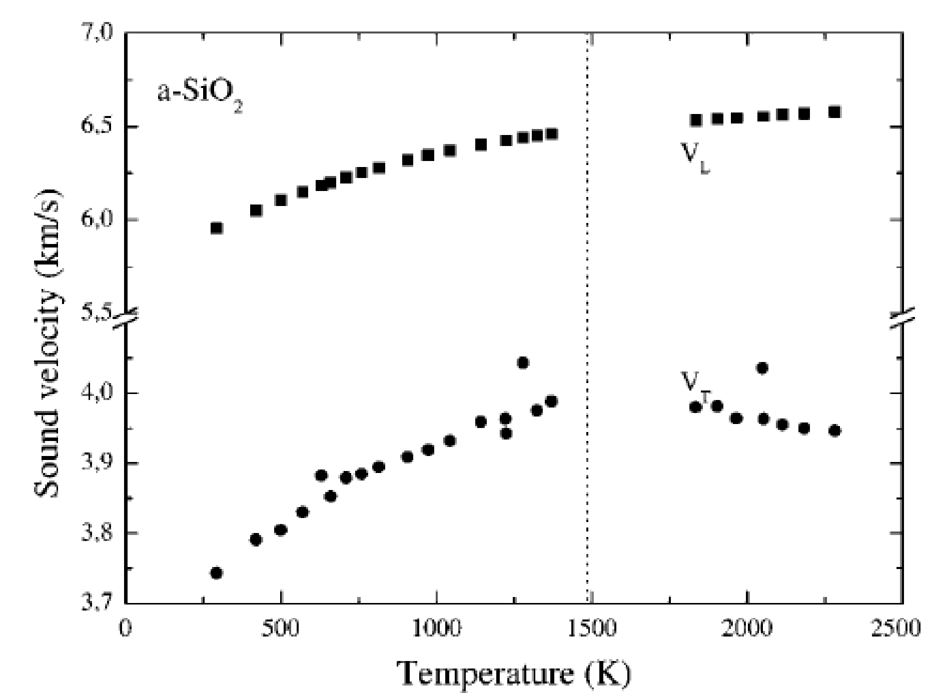

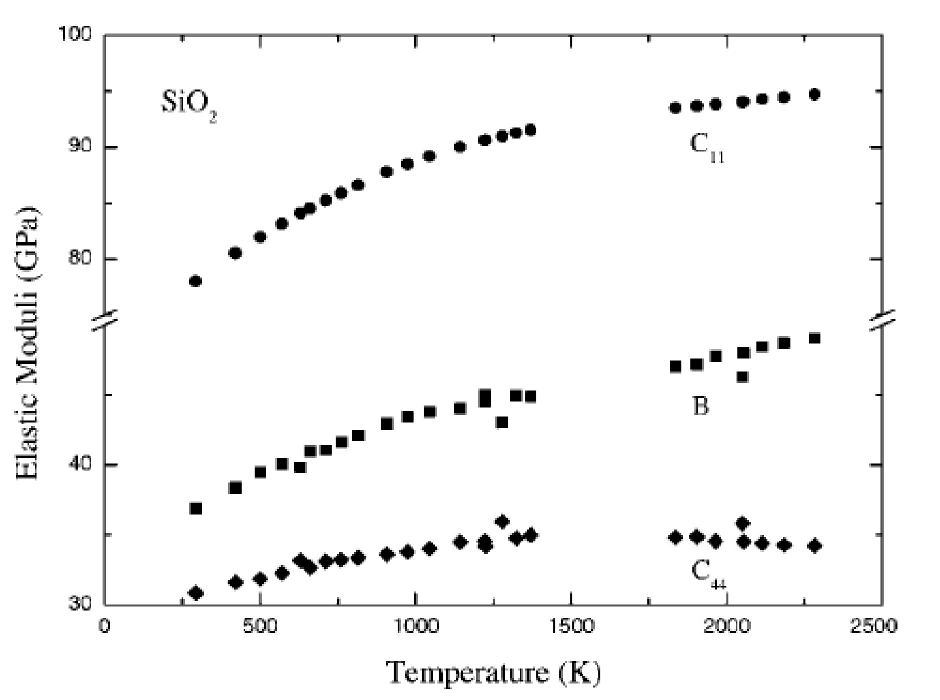

Haplogranite glasses (NAS)

[A. Hushur *et al* Am. Min. 2013]

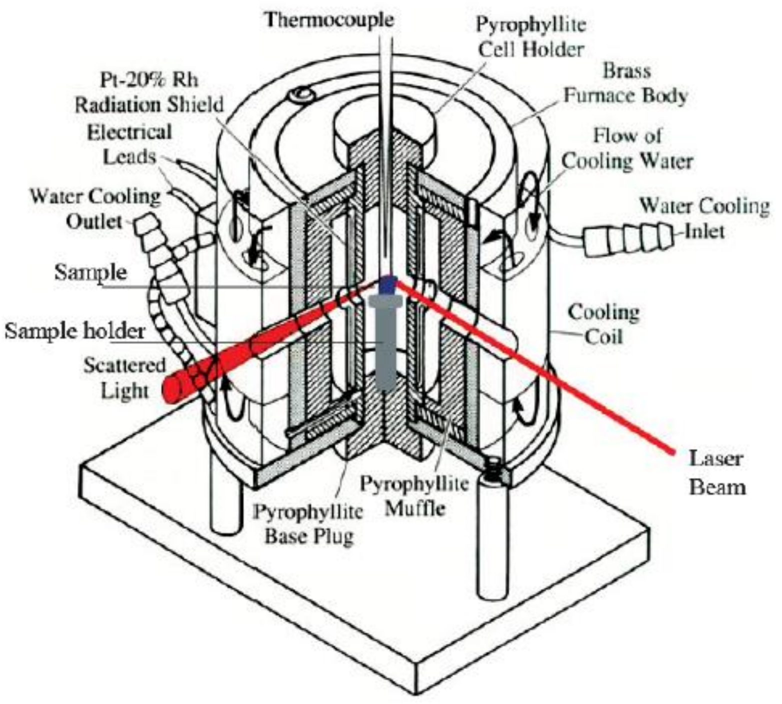

FIGURE 1. Cross section of the high-temperature furnace used for Brillouin spectroscopy. Two Pt-Pt 10% Rh (Type S) thermocouples were used to measure the temperature. One rests slightly against the sample and one is attached to the sample holder. (Color online.)

Backscattering and platelet geometries

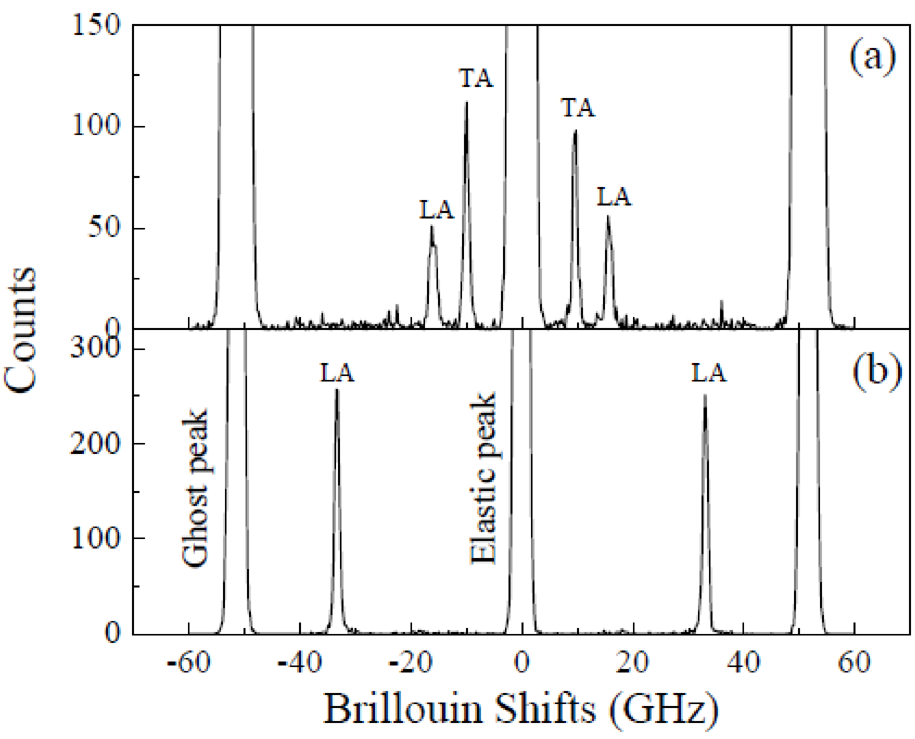

FIGURE 2. A typical Brillouin spectrum measured in (**a**) right-angle scattering geometry and (**b**) backscattering geometry. LA indicates the longitudinal acoustic phonon, while TA is the transverse acoustic phonon.

Haplogranite glasses (NAS)

[A. Hushur *et al* Am. Min. 2013]

Oxide composition (wt%)	HPG8_Li05	HPG8_F05
SiO_2	73.2(3)	77.0(2)
Al_2O_3	12.9(3)	11.1(1)
Na_2O	4.3(3)	4.5(1)
K_2O	4.4(2)	4.1(1)
Li_2O	4.9(4)	0.000
F	0.000	4.6(1)
Total	99.7	101.3

n(T) from both geometries

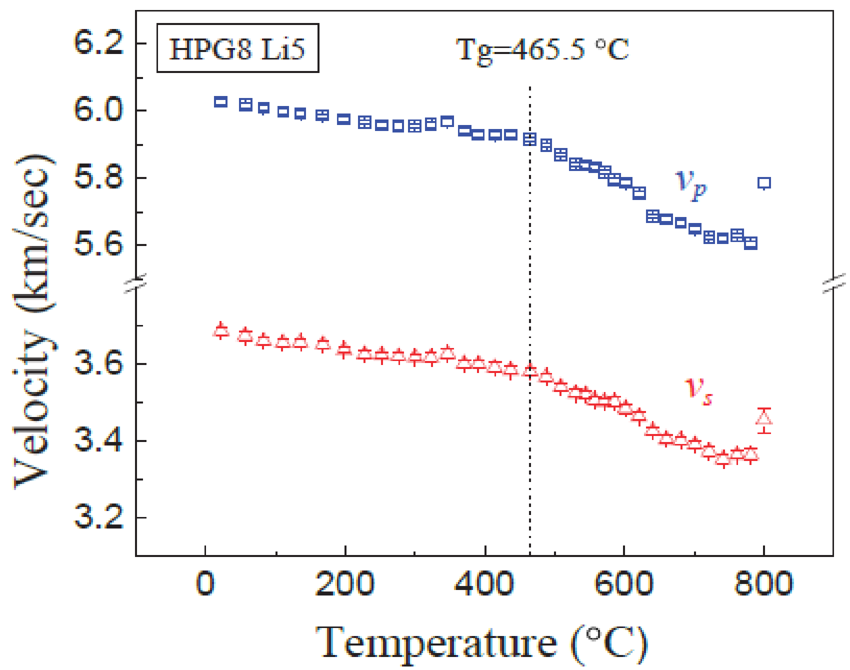

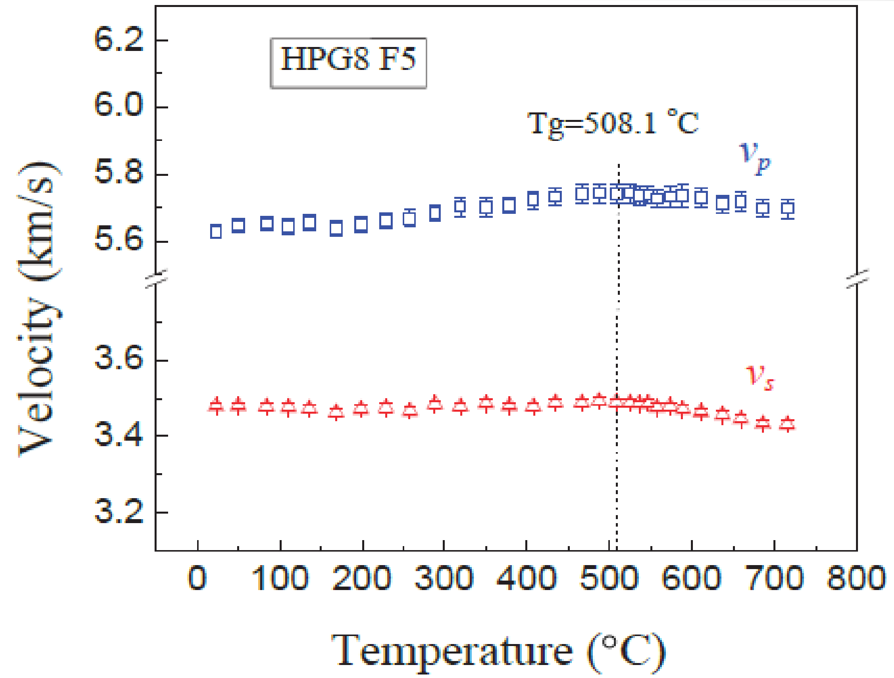

Haplogranite glasses (NAS)

[A. Hushur *et al* Am. Min. 2013]

ρ from Lorentz-Lorenz formula

$$(n^2 - 1)/(n^2 + 2) = 4\pi\alpha\rho/(3M),$$

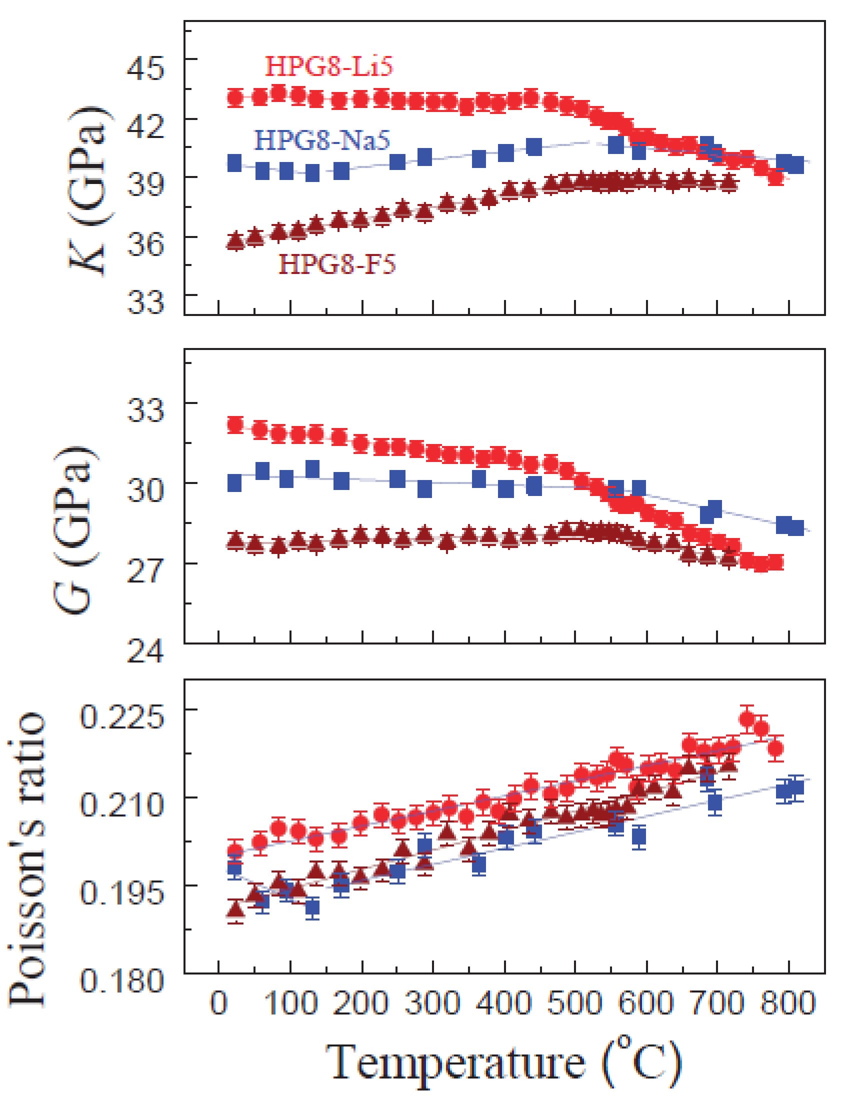

TABLE 1. ICP-AES chemical compositions of the four anhydrous haplogranite samples (wt%)

Oxide composition (wt%)	HPG8_Li05	HPG8_Na05	HPG8_K05	HPG8_F05
SiO_2	73.2(3)	74.1(4)	74.6(8)	77.0(2)
Al_2O_3	12.9(3)	11.7(6)	11.8(8)	11.1(1)
Na_2O	4.3(3)	9.0(2)	4.4(8)	4.5(1)
K_2O	4.4(2)	4.4(9)	9.2(10)	4.1(1)
Li_2O	4.9(4)	0.000	0.000	0.000
F	0.000	0.000	0.000	4.6(1)
Total	99.7	99.2	100.0	101.3

Note: Standard deviations are given in parentheses.

Outline

- Introduction
- Brillouin scattering mechanism
- Instrumentation
- **Applications to melts**

Viscoelasticity in oxide melts

Shear modes in B_2O_3 up to 1270 K
(T_g = 523 K, T_m = 723 K) ➡ 2 T_m

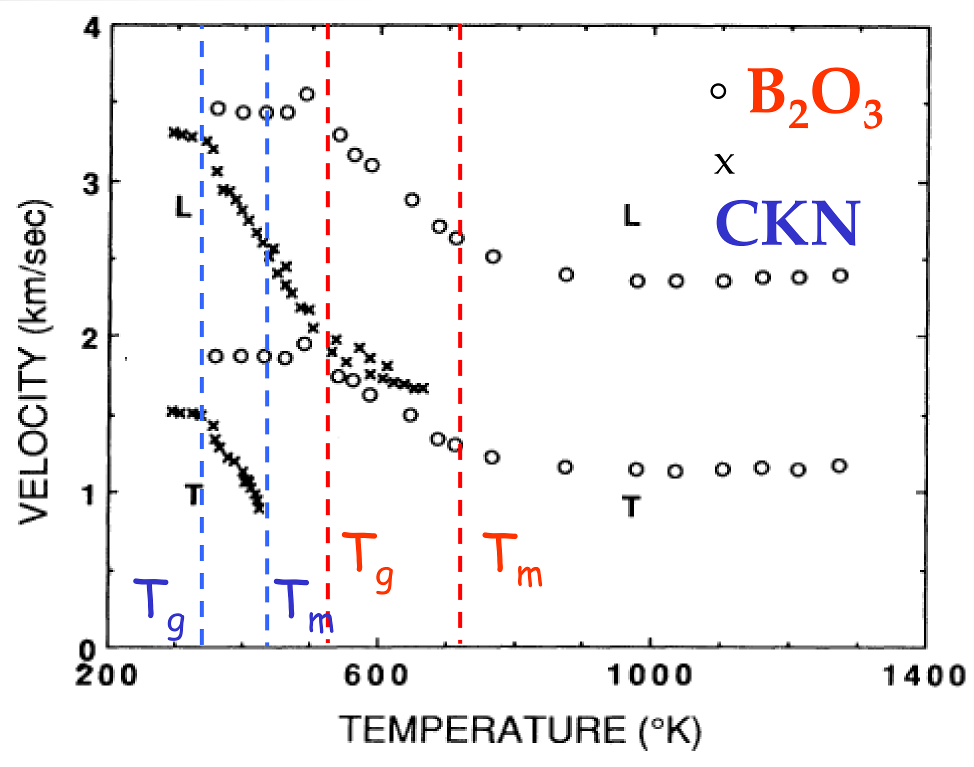

M. Grimsditch, R. Bhadra, and L. M. Torell, PRL (1989)

1300 K

$$\tau_s^{-1} = 0.25\,\text{GHz} < \nu_B^T \approx 4.5\,\text{GHz}$$

$$\eta_s \approx 10^2\ \text{Pa.s}$$

$Ca_{0.4}K_{0.6}(NO_3)_{1.4}$

ν_B^T not measureable at T_m

Glycerol case

[L. Comez *et al* J. Chem. Phys. 2003]

T_g ~ 187 K T_m ~ 291 K

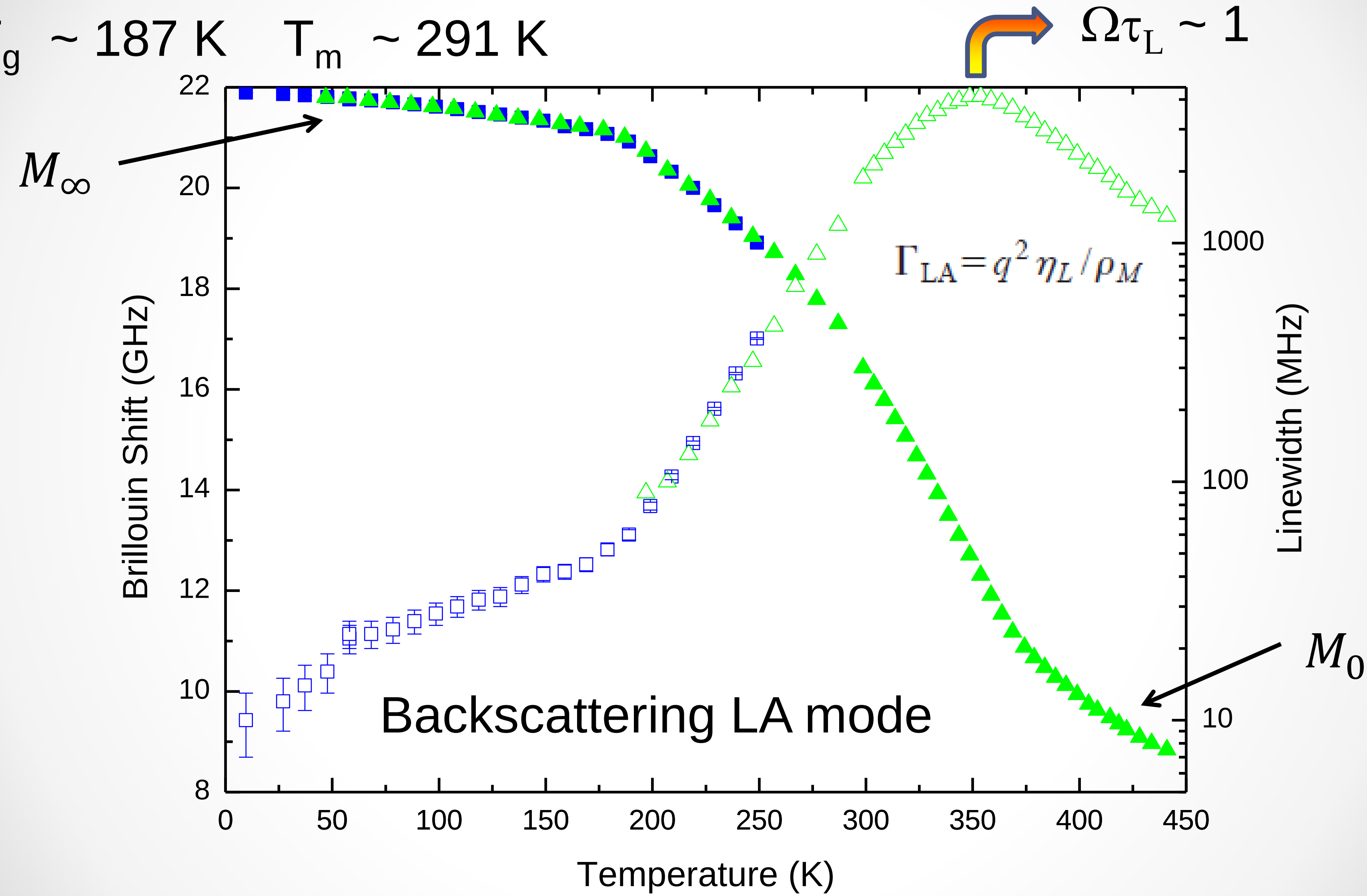

Glycerol case

[L. Comez *et al* J. Chem. Phys. 2003]

Data analysis using generalized hydrodynamics

$$S(q,\omega)=\frac{S(q)M}{\pi\omega}\,\frac{M''(\omega)}{[\omega^2\rho_M/q^2-M'(\omega)]^2+[M''(\omega)]^2}$$

$$M(\omega)=M_\infty+\Delta M(\omega)+i\omega\eta_\infty$$ L

$$\Delta M(\omega)=(M_0-M_\infty)/(1+i\omega\tau)$$

M'' shows a peak at $\tau^{-1}=\omega$

$$\Delta M(\omega)=(M_0-M_\infty)/(1+i\omega\tau)^\beta$$

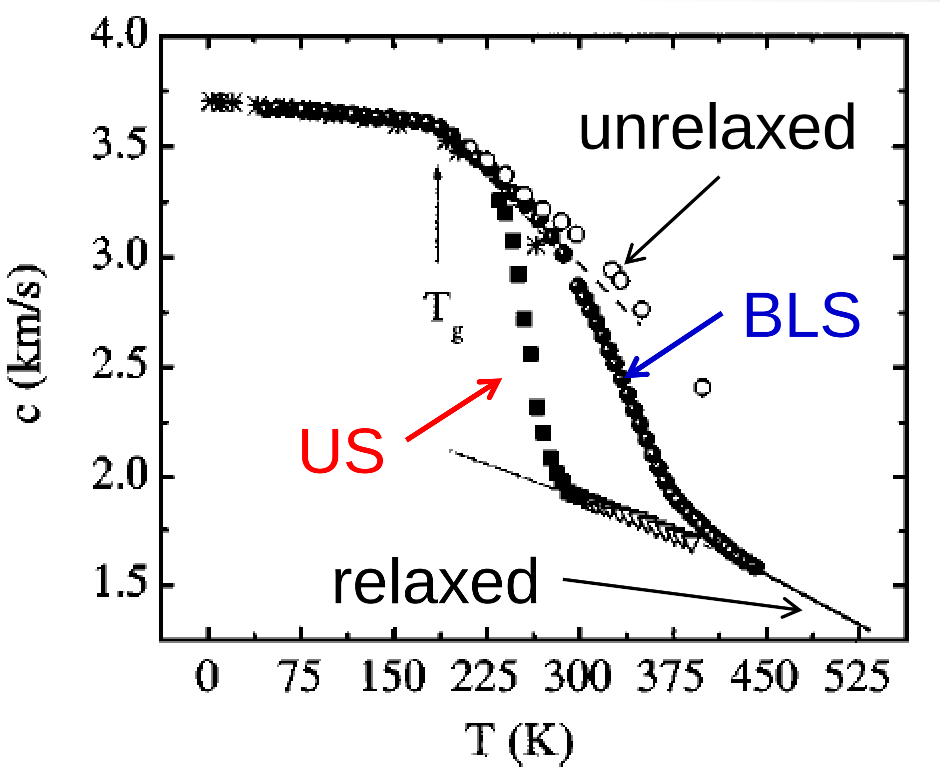

$$\omega_{LA}=q(M/\rho_M)^{1/2}$$

$$\Gamma_{LA}=q^2\eta_L/\rho_M$$